Chronology of the Saxothuringian subduction in the West Sudetes (Bohemian Massif, Czech Republic and Poland)

Jiří Konopásek[1,2], Robert Anczkiewicz[3], Petr Jeřábek[4], Fernando Corfu[5], Eliška Žáčková[2]

[1] Department of Geosciences, UiT – The Arctic University of Norway in Tromsø, Dramsveien 201, N-9037 Tromsø, Norway

[2] Czech Geological Survey, Klárov 3, 118 21 Prague 1, Czech Republic

[3] Institute of Geological Sciences, Polish Academy of Sciences, Kraków Research Centre, Senacka 1, 31-002 Kraków, Poland

[4] Institute of Petrology and Structural Geology, Faculty of Science, Charles University in Prague, Albertov 6, 128 43 Prague, Czech Republic

[5] Department of Geosciences and CEED (Centre for Earth Evolution and Dynamics), University of Oslo, P.O. Box 1047, Blindern, 0316 Oslo, Norway

Abstract

Isotopic dating of monazite and garnet from high-pressure metamorphic rocks exposed in the northern part of the Saxothuringian paleo-suture in the Bohemian Massif revealed a diachronous metamorphism of various rock types that are now closely associated within allochthonous units representing the Devonian–Carboniferous subduction–accretionary complex. Mafic blueschists of the middle unit yielded a Lu–Hf garnet age of 363.9 ± 1.3 Ma. The blueschists occur within high-pressure, garnet-free phyllites. Monazite extracted from this rock-type yielded a U–Pb ID–TIMS age of 336.5 ± 0.5 Ma. Garnet-bearing micaschist of the lower unit contains monazite with a U–Pb SIMS age of 341 ± 3 Ma, consistent with Lu–Hf garnet-whole rock ages of 344.5 ± 1.3 and 342 ± 7 Ma obtained from the same rock type.

Existing tectonic models of the Bohemian Massif, and particularly of its northern part, assume that the period of oceanic subduction was terminated at *c.* 380–375 Ma by the arrival of an attenuated Saxothuringian continental crust, which was partly subducted and partly relaminated underneath the overriding Teplá–Barrandian Domain. However, our data, as well as data from mafic high-pressure rocks in the southern part of the Saxothuringian domain suggest that the initial collision was probably caused by the arrival of a smaller crustal block present within the Saxothuringian oceanic domain. After its subduction and relamination, the oceanic subduction was re-established and terminated by continental subduction and later collision of the Saxothuringian passive margin at *c.* 345–335 Ma.

Key words: geochronology, high-pressure metamorphism, subduction, Variscan, Bohemian Massif

Introduction

Subduction of the Saxothuringian Ocean together with the leading edge of the Saxothuringian continental crust is regarded as the driving force for the Devonian–Carboniferous tectonic evolution of the Bohemian Massif (Fig. 1; e.g. Matte *et al.* 1990; Franke 2000; Konopásek & Schulmann 2005; Schulmann *et al.* 2009; 2014). Along-strike changes in metamorphic conditions along the Saxothuringian paleo-suture suggest different exhumation levels of the allochthonous units present in its southwestern (the Erzgebirge) and northeastern (the West Sudetes) parts (Fig. 1). The southwestern segment preserves medium- to high-temperature eclogites and high-pressure granulites (Schmädicke *et al.* 1992; Klápová *et al.* 1998; Nasdala & Massonne 2000; Kotková *et al.* 1996; 2011; Collet *et al.* 2017), whereas in the northeast the high-pressure conditions are recorded only in low-temperature metamorphic rocks (Cháb & Vrána 1979; Guiraud & Burg 1984; Kryza *et al.* 1990; Smulikowski 1995; Patočka *et al.* 1996; Žáčková *et al.* 2010; Faryad & Kachlík 2013; Jeřábek *et al.* 2016; Majka *et al.* 2016). For this reason, the time span of the Saxothuringian subduction is better understood in the southwest, along the Saxothuringian – Teplá-Barrandian Domain interface, where the higher temperature conditions allowed linking the crystallization of minerals suitable for geochronology with the metamorphic peak and subsequent exhumation. Such data have shown two periods of peak metamorphism and exhumation of the high pressure rocks, one in the late Devonian and the other in the early Carboniferous (Stosch & Lugmair 1990; Beard *et al.* 1995; Kotková *et al.* 1996; 2016; Kröner & Willner 1998; von Quadt & Günther 1999; Werner & Lippolt 2000; Zulauf *et al.* 2002; Timmermann *et al.* 2004; Mlčoch & Konopásek 2010; Konopásek *et al.* 2014; Collett *et al.* 2018), suggesting at least a 50 my lifetime of the subduction process.

In the West Sudetes, the low metamorphic temperatures of the high-pressure rocks were causing problems in understanding of the temporal evolution of the subduction-related nappe stack. Up to now, the only available geochronological data were the Ar–Ar ages from the mafic blueschists and from associated metasedimentary rocks (Maluski & Patočka 1997; Marheine *et al.* 2002).

Although these data suggested that there could be an important diachronism in the timing of metamorphism within the subduction channel, it was assumed that the older, late Devonian age represents the timing of the high-pressure metamorphism, whereas the early Carboniferous ages represent the greenschist facies overprint associated with exhumation of the nappe stack (Maluski & Patočka 1997; Mazur & Aleksandrowski 2001; Marheine *et al.* 2002). Later on, Žáčková *et al.* (2010) documented an evidence for early Carboniferous high-pressure metamorphism in the southern part of the West Sudetes, though their age estimates involved rather large errors.

Jeřábek *et al.* (2016) have suggested a two-stage tectonic evolution of the Krkonoše-Jizera Massif in the West Sudetes (Fig. 2). In the early stage, the high-pressure metamorphism was accompanied by stacking of nappe sheets within the subduction channel resulting in juxtaposition of rock units that were metamorphosed at different depths and possibly also in different periods of the lifetime of the subduction zone. The second stage was interpreted as a result of the transition from subduction towards the collisional stage of the convergent evolution. This stage was associated with extrusion of the rocks from the subduction channel and large-scale folding of the earlier developed nappe stack. The timing of particular tectonic processes is not clear, mainly due to the fact that, except for the monazite data by Žáčková *et al.* (2010), only Ar–Ar ages are available for the various rock-types of the particular nappes in the the Krkonoše-Jizera Massif. The data span the entire interval between *c.* 360 and 315 Ma (Maluski & Patočka 1997; Marheine *et al.* 2002) and in many cases it is difficult to discern whether they represent the timing of formation or cooling of the dated minerals.

In this work, we provide high precision ages of minerals interpreted as members of the high-pressure metamorphic mineral assemblages of basic igneous and clastic sedimentary rocks of the Krkonoše-Jizera Massif. The isotopic systems used for the dating (U–Pb and Lu–Hf) have substantially higher closure temperatures than the estimated peak metamorphic conditions of the studied samples, so there is little doubt that the ages represent the timing of crystallization of the high-pressure mineral assemblages. We link the obtained ages with our recently published geodynamic model of the evolution of the high-pressure nappe stack in the Krkonoše-Jizera Massif (Jeřábek *et al.* 2016) and provide additional evidence that the geodynamic evolution of the northeastern and southwestern segment of the Saxothuringian paleo-suture in the Bohemian Massif is indeed very similar.

Geological setting

The West Sudetes (Franke *et al.* 1993; Narębski 1994; Franke & Żelaźniewicz 2000) represent the northernmost exposed part of the Saxothuringian Domain in the Bohemian Massif (Figs. 1 and 2). The southern part of the West Sudetes is represented by the Krkonoše-Jizera Massif (Fig. 2), interpreted as a subduction–accretionary complex related to the Devonian subduction of the Saxothuringian Ocean and subsequent underthrusting of the Saxothuringian continental margin below the Teplá-Barrandian Domain s.l. (Mazur & Aleksandrowski 2001). The core of the Krkonoše-Jizera Massif is built of (meta)granitoid rocks with Early Palaeozoic protolith ages (Borkowska *et al.* 1980; Korytowski *et al.* 1993; Oliver *et al.* 1993; Kröner *et al.* 2001) surrounded by metamorphosed volcanosedimentary rocks interpreted as former Early Paleozoic cover of the Saxothuringian passive margin laid down during intracontinental rifting and the subsequent opening of the Saxothuringian Ocean (Kryza *et al.* 1995, 2007; Winchester *et al.* 1995, 2003; Kachlík & Patočka 1998; Patočka *et al.* 2000; Dostál *et al.* 2001; Žáčková *et al.* 2012). The convergent evolution started with subduction of the Saxothuringian Ocean and associated passive margin deposits accompanied by a development of high-pressure mineral assemblages in both mafic (Cháb & Vrána 1979; Guiraud & Burg 1984; Kryza *et al.* 1990; Smulikowski 1995; Faryad & Kachlík 2013; Majka *et al.* 2016) and felsic (Žáčková *et al.* 2010; Jeřábek *et al.* 2016) lithologies. The subsequent collisional stage resulted in the exhumation of high-pressure rocks from the subduction channel, their extensive retrogression under greenschist facies conditions and post-metamorphic folding of the entire metamorphic complex. In the late stages of the tectonic evolution at *c.* 320–312 Ma, the Krkonoše-Jizera Massif was intruded by the Krkonoše-Jizera Plutonic Complex (Machowiak & Armstrong 2007; Žák *et al.* 2013; Kryza *et al.* 2014).

Žáčková *et al.* (2010) distinguished four tectonic units in the Krkonoše-Jizera Massif. The par-autochthonous basement comprises (meta)granitoid rocks of the Lusatian and Jizera massifs that show Neoproterozoic–Late Cambrian/Early Ordovician protolith ages (Kröner *et al.* 1994; Tichomirowa *et al.* 2001). In the westernmost part of the Krkonoše-Jizera Massif, the (meta)granitoid complex is covered by very low-grade Neoproterozoic–Lower Palaeozoic sedimentary rocks of the Ještěd Unit (Chaloupský 1989; Chlupáč 1993; Kachlík & Kozdrój 2001). Structurally above is the lower allochthonous unit built of ± garnet-bearing micaschists accompanied by a thick orthogneiss body, subordinate quartzite and marble bodies (Fig. 2). Based on geochemistry, Winchester *et al.* (2003) interpreted the sedimentary protolith of the micaschists as a proximal facies of the former passive margin. High-pressure metamorphism that reached upper blueschist facies conditions has been recognized in the micaschists of the lower unit by Žáčková *et al.* (2010). The middle allochhonous unit is represented by garnet-free micaschists, phyllites and marbles (Fig. 2), which were interpreted by Winchester et al. (2003) as a former distal facies of the Saxothuringian passive margin. This unit contains numerous bodies of metamorphosed mafic rocks showing relics of blueschist facies mineral assemblages (Cháb & Vrána 1979; Guiraud & Burg 1984; Kryza & Mazur 1995; Smulikowski 1995; Patočka *et al.* 1996; Majka *et al.* 2016). Due to the presence of high-pressure metamorphism, the rocks of the lower and middle units are regarded as the association exhumed from the subduction channel (Mazur & Aleksandrowski 2001; Jeřábek *et al.* 2016). The upper unit is the Leszczyniec Complex (Fig. 1) dominated by metabasic rocks. This unit has been interpreted by Mazur & Aleksandrowski (2001) as a remnant of the floor of the Saxothuringian Ocean attached to the upper (Teplá–Barrandian) plate in early stages of the subduction process, as it does not show signs of high pressure metamorphism (Kryza & Mazur 1995).

The structural order of the lower, middle and upper units is preserved in its normal position only in the eastern Krkonoše-Jizera Massif (Fig. 2). The simple nappe structure and spatial distribution of the lower and middle units become complicated towards the west as a result of two subsequent stages of folding (Jeřábek *et al.* 2016). The earlier folding led to the development of two mega-scale recumbent isoclinal folds, which in the central part of the Krkonoše-Jizera Massif brought the tectonic contact between the middle and lower units into an overturned position (Fig. 2). Further to the west, the order of the units becomes normal again, with the lower unit in the structural hanging wall of the par-autochthon and in the footwall of the middle unit. The tectonic contact between the lower and middle units has been previously interpreted as the Saxothuringian suture (Mazur *et al.* 2001; 2006). However, as the work of Žáčková *et al.* (2010) has shown that both the lower and middle units underwent blueschist-facies metamorphism, the presumed suture is likely located higher up in the nappe pile between the middle and upper (Leszczyniec Complex) units.

Sample description and the results of the isotopic dating of monazite

In order to determine the timing of metamorphism in the high-pressure units of the Krkonoše-Jizera Massif, four samples were collected for U–Pb dating of metamorphic monazite and/or for Lu–Hf dating of garnet. Dating of monazite was carried out by the Secondary Ion Mass Spectrometry (SIMS) at the NORDSIM laboratory in Stockholm or by Isotope Dilution Thermal Ionisation Mass Spectrometry (ID–TIMS) at the Department of Geosciences of the University of Oslo. Description of the analytical methods is provided in the “Appendix”.

Samples VU 600 and VU 602

Samples VU 600 (N 50.71870°, E 15.76628° - all coordinates are in WGS84) and VU 602 (N 50.74171°, E 15.79940°) represent the garnet micaschist of the lower unit (Fig. 2). Both samples consist of garnet–chlorite–biotite–white mica–quartz–ilmenite. Garnet is subhedral in shape, in some places partly replaced by biotite along the margins. Some of the garnet porphyroblasts are poikilitic with inclusions commonly represented by quartz and elongated ilmenite crystals (Fig. 3a). Metamorphic conditions of equivalent micaschist samples from the lower unit were estimated at c. 460–520°C and 18–19 kbar for the onset of garnet growth and at c. 470–520°C at 10.5–13.5 kbar for the matrix mineral assemblage (Žáčková *et al.* 2010). Accessory monazite occurs within the white mica-rich bands aligned parallel with the foliation and it is interpreted as being stable with the matrix mineral assemblage (Fig. 3a).

Monazite separated from sample VU 602A are elongated tabular crystals usually *c.* 60–80 μm long and showing zones enriched in Th and other zones with slight enrichment in La (Fig. 4; Tab. 1). SIMS isotopic analysis of the monazite has revealed that the crystals are isotopically homogeneous. Eighteen analyses (Tab. 2) obtained from six grains combine in a concordia U–Pb age of 341 ± 3 Ma (2 sigma error; Fig. 5a), which is interpreted as the best estimate for the timing of stabilization of the matrix mineral assemblage.

Sample EL 9/2

Sample EL 9/2 (N 50.66015°, E 15.26154°) is a fine-grained phyllite of the middle unit (Fig. 2) containing the mineral assemblage chloritoid–chlorite–white mica–quartz (Fig. 3b). Conditions of stabilization of this assemblage were estimated at c. 400–450°C and 14–16 kbar (Jeřábek *et al.* 2016).

The sample contains accessory monazite that is *c.* 30–60 μm large. It forms isometric or elongated grains oriented parallel with the foliation and rich in micron-sized inclusions (Fig. 3b). The crystals show Th-, Nd-, Sm- and Gd-rich cores and La-rich rims (Fig. 4; Tab. 1). In mineral separates they occur typically as rather rusty and externally altered grains. The attempt to apply air abrasion to remove this alteration had to be abandoned because the grains proved to be very brittle and disintegrated easily. Therefore the ID-TIMS analyses (Tab. 2) were conducted on unabraded monazite, either single grains or fractions of small fragments selected among the most clear and transparent ones. Five of them yielded concordant and overlapping results, which combine into a concordia U–Pb age of 336.5 ± 0.5 Ma (2 sigma error; Fig. 5b). One analysis (Tab. 2) of several small grains is slightly discordant and younger; these grains were presumably affected by the alteration evident in some of the grains. The age of 336.5 ± 0.5 Ma is interpreted as the timing of stabilization of the matrix mineral assemblage.

Sample VU 601

Sample VU 601 (N 50.69704°, E 15.86115°) is a garnet-bearing blueschist collected at the Kopina hill locality situated in the eastern part of the Krkonoše-Jizera Massif at the border between the Czech Republic and Poland (Fig. 2). In the work of Jeřábek *et al.* (2016), the occurrences of the mafic blueschists were considered as a part of the rock assemblage representing the middle unit. The sample consists of *c.* 1 mm large, euhedral to subhedral garnet crystals surrounded by a fine-grained matrix represented by epidote, glaucophane, Ca-amphibole, titanite, quartz, hematite, ± carbonate and secondary chlorite (Fig. 3c). Ilmenite and epidote also occur as inclusions in the garnet. Metamorphic conditions of the Kopina blueschist were estimated at 12–15 kbar and 480–520°C by Majka *et al.* (2016).

Results of Lu–Hf garnet dating

Lu–Hf results are summarized in Tab. 3 and Fig. 6. Due to the relative ease of garnet separation we analysed three garnet aliquots from sample VU 600, while only two garnet aliquots were prepared from the remaining samples. For each sample, representative whole rock powder was analysed for the initial $^{176}Hf/^{177}Hf$ ratio correction. Garnet mica schist samples VU 600 and VU 602 yielded ages of 342 ± 7 and 344.5 ± 1.3 Ma, respectively, and these are considered equivalent within their analytical errors. Garnet bearing blueschist sample VU 601E gave a significantly older age of 363.9 ± 1.3 Ma (Fig. 6).

In both micaschist samples the garnet shows rather high Hf contents (1.3–1.9 ppm) determined by the isotope dilution analysis (Tab. 3). These values are much higher than those typical of metamorphic garnets from average metapelitic rocks (e.g. Scherer *et al.* 2000; Anczkiewicz *et al.* 2004, 2014; Platt *et al.* 2006). More significantly, however, the values are much higher than Hf concentration in the inclusion-free parts of garnet, which were estimated by LA ICP-MS to be *c.* 50 ppb (Fig. 7a, d). Obviously, the isotope dilution analyses were influenced by Hf-rich inclusions, most likely ilmenite, which is particularly abundant in garnet from the micaschist samples (Fig. 3a). Because ilmenite apparently crystallized in equilibrium with the surrounding garnet, its presence did not distort accuracy of our analyses. Some Hf peaks visible in the traverses across the garnet crystals in the micaschist samples are due to ilmenite and apatite inclusions as indicated by the good correlation of the Hf spikes with Ti or P spikes (Fig. 7c, f). Some Hf spikes correlate well with the spikes of U, which largely originates from apatite inclusions, but could also be partly derived from metamict zircon crystals which despite hot-plate dissolution may release Hf (Fig. 7b, e). As the rocks were metamorphosed at relatively low T (*c.* 500°C), zircon occurs only as detrital, inherited crystals and hence their contribution to the Lu–Hf budget would particularly influence the accuracy of dating results. Although some limited contribution to the Hf budget from zircon cannot be ruled out, it seems to be of very minor significance taking into account the good consistency with the monazite ages presented above. Only the Grt2 fraction, which contributes significantly to the “excess” scatter (MSWD = 3.4) of VU 600 (Tab. 3), may reflect a zircon effect.

Isotope dilution analyses of garnet-bearing blueschist sample VU 601E show Hf concentration in garnet at the level of about 100 ppb, which is commonly observed in metamorphic rocks. Still, this is somewhat higher than our LA ICP-MS analyses indicating Hf abundance at the level of *c.* 50 ppb. In our view, minor Hf contamination was most likely caused the by the main rock forming minerals (inclusions or intergrowths), rather than by Hf-rich inherited phases which would considerably lower the $^{176}Lu/^{177}Hf$ ratios (Fig. 6 and Tab. 3).

Lu concentrations in all the studied samples correspond well with an average Lu concentration determined by LA ICP-MS. Lu zonation profiles presented in Fig. 7a, d, g show fairly typical, and qualitatively nearly identical, prograde zonation expressed by the highly enriched cores and the Lu-poor rims. All three samples show a “bulge” expressed to variable degrees about half way between core and rim suggesting oscillatory type zonation.

Taking into account the prograde Lu zonation in garnet and overall low crystallization temperature of all three samples, we interpret the obtained Lu–Hf garnet ages as reflecting the time of prograde garnet formation. Noteworthy, the time span between early garnet formation and metamorphic peak was probably very small. Garnet most likely nucleated near 500°C, and since these rocks have never reached much higher temperatures, metamorphic peak must have quickly followed the stage of an early garnet formation.

Discussion

Timing of high-pressure metamorphism and tectonic subdivision of the Krkonoše-Jizera Complex

Samples VU 600 and VU 602 represent garnet-bearing micaschist of the lower unit in the Krkonoše-Jizera Complex nappe stack. Previous dating of the monazite from the same unit and rock type provided a LA ICP-MS age of 328 ± 6 (2 sigma) Ma and electron microprobe chemical dating yielded an age of 330 ± 10 (95% conf.) Ma (Žáčková *et al.* 2010). Even though the LA ICP-MS age was calculated from dates with rather low equivalence and the electron microprobe dating had an elevated analytical uncertainty, the data for the first time suggested that the high-pressure metamorphism in the Krkonoše-Jizera Complex, until then believed to be Devonian in age (Maluski & Patočka 1997), may be diachronous. One muscovite sample of Marheine *et al.* (2002) collected within the lower unit (SK201) yielded an Ar–Ar age of 340 ± 6 Ma, it was however interpreted as representing the timing of collision-related recrystallization.

Our ages obtained by two independent chronometers confirm an early Carboniferous age of the high-pressure metamorphism of the lower unit micaschists, however the resulting ages are *c.* 15 my older than the previous estimates by Žáčková *et al.* (2010). The garnet, which has been interpreted by Žáčková *et al.* (2010) as a part of the high-pressure mineral assemblage, yielded the Lu–Hf ages of 342 ± 7 and 344.5 ± 1.3 Ma. Due to strong Lu enrichment in garnet core, our Lu–Hf dates are shifted towards early garnet growth (Lapen *et al.* 2003), and thus are interpreted as dating an early high pressure phase of metamorphism at about 345 Ma (the precise age obtained for garnet from sample VU 602). Žáčková *et al.* (2010) documented the presence of monazite both within the garnet and in the matrix, which also suggests its stability during the high-pressure metamorphism. The U–Pb isotopic dating of the monazite yielded an age of 341 ± 3 Ma. The Y content in monazite is slightly lower than in garnet core but much higher than in garnet rim (Tab. 4, Fig. 7), whereas the contents of heaviest REEs (Yb, Lu) in monazite are much lower than in garnet core but similar to those in garnet rim (Tab. 4, Fig. 8). This suggests that monazite crystallized possibly slightly later than garnet core but still during garnet growth. This is in accord with observations by Žáčková *et al.* (2010), who observed monazite within garnet of the lower unit micaschists about half way between core and rim. Such geochemical signature explains the slightly younger monazite age. The overlap of the ages within their analytical errors, as well as the use of two independent chronometers suggest that the time interval of *c.* 340–345 Ma represents a robust estimate of the timing of high-pressure metamorphism in the micaschists of the lower unit in the Krkonoše-Jizera Complex.

Samples VU 601 and EL9/2 represent mafic blueschist and chloritoid phyllite, respectively. In our previous work (Jeřábek *et al.* 2016), these two lithologies were both regarded as representing the middle unit of the Krkonoše-Jizera Complex nappe stack due to unclear timing of metamorphism in the garnet-free phyllites. Dating of phengitic potassium white mica from a sample of garnet-free mafic blueschist in the easternmost part of the Krkonoše-Jizera Complex by Maluski & Patočka (1997) provided an Ar–Ar age of 364 ± 2 Ma, which was interpreted as the age of high-pressure metamorphism. This age is now matched by our Lu–Hf age of 364 ± 1 Ma for garnet from a rare locality of garnet-bearing mafic blueschist within the same unit. The monazite grains from the chloritoid phyllite of the middle unit yielded the U–Pb age of 336.5 ± 0.5 Ma, which contrasts with the *c.* 30 my older age of metamorphism of the associated mafic blueschists. On the other hand, the monazite age of the chloritoid phyllite is *c.* 20 my older than the majority of Ar–Ar ages obtained from samples of the middle unit by Marheine *et al.* (2002). Thus, the isotopic dating of minerals representing the high-pressure assemblages shows that the middle unit is a composite sheet made up of rocks with different metamorphic histories.

Duration and dynamics of the Saxothuringian subduction zone in the West Sudetes

The results of isotopic dating of high-pressure mineral assemblages preserved in the studied samples confirm the interpretation of Žáčková *et al.* (2010) that the blueschist facies rocks of the Krkonoše–Jizera Complex record different periods in the lifetime of the Saxothuringian subduction zone. This finding contrasts with the interpretation of the Ar–Ar dates for amphiboles and micas from rocks of the Krkonoše–Jizera Complex by Maluski & Patočka (1997) and Marheine *et al.* (2002), who suggested that subduction had terminated at, or shortly after, *c.* 364–359 Ma and the majority of the ages between *c.* 344 and 333 Ma represent a collision-related greenschist facies overprint. Published metamorphic data and the new geochronological data suggest active subduction at least between *c.* 364 Ma and 337 Ma. The revised estimates of metamorphic conditions from the

Krkonoše-Jizera Complex blueschist by Majka *et al.* (2016) suggested peak pressures of *c.* 12–15 kbar at temperatures of *c.* 480–520°C. The data from the metasedimentary rocks of the lower and middle units show even higher depth of burial corresponding to *c.* 14–19 kbar at temperatures of *c.* 450–520°C with slightly lower pressure conditions determined for phylites in the middle unit suggesting a normal metamorphic field gradient in the exhumed nappe stack (Žáčková *et al.* 2010; Jeřábek *et al.* 2016).

The set of metamorphic and geochronological data allows for a more detailed characterization of the dynamics of the Saxothuringian subduction zone in the area of the West Sudetes. The oldest subduction-related event is recorded by the stabilization of the garnet-bearing high-pressure mineral assemblage in the mafic blueschist at *c.* 365 Ma. Analysis of the metamorphic evolution of this rock-type by Majka *et al.* (2016) suggests prograde growth of garnet between *c.* 480 and *c.* 520°C at depths between *c.* 45 and 55 km (Fig. 9a), which corresponds to an established thermal gradient of 9–10°C/km. As these are the estimated maximum metamorphic conditions, it is expected that at *c.* 365 Ma the unit of the mafic blueschists was decoupled from the subducting slab (Fig. 9a) and either attached to the upper plate, or it was partly exhumed during the following continental subduction (Fig. 9b). The fate of the mafic blueschists during the following *c.* 25 my is difficult to constrain, because there are no age data for the development of the retrogressive greenschist facies assemblages.

High-pressure mineral assemblages in metamorphosed clastic sediments of the lower and middle units (described by Winchester *et al.* (2003) as former proximal and distal sedimentary sequences of the Saxothuringian passive margin, respectively) are interpreted as documenting the transition from oceanic to continental subduction (Fig. 9b). The data of Jeřábek *et al.*, (2016) suggest that the depth reached by the middle unit was *c.* 55–70 km and there seems to be a lateral variation in peak metamorphic temperature for the sample collected in the eastern (*c.* 450–500°C) and in the western parts of the unit (*c.* 400–440°C). The rocks of the lower unit reached greater depth (*c.* 70–75 km) and equilibrated at temperature of *c.* 450–500°C (Žáčková *et al.* 2010). The estimated peak pressure conditions in metamorphic rocks of the middle and lower unit suggest cooling of the subduction channel and related drop of the thermal gradient from *c.* 9–10°C/km at *c.* 365 Ma to *c.* 8–6°C/km at *c.* 340 Ma (Fig. 9b).

The metasedimentary rocks of the lower and middle units must have been detached from the down-going continental margin after reaching their metamorphic peak. Metamorphic data from the rocks of the lower unit show an important period of nearly isothermal decompression, suggesting a first stage of exhumation of this unit within the subduction channel (Žáčková *et al.* 2010). Jeřábek *et al.* (2016) interpreted this early exhumation as a period when the mafic blueschists, middle and lower units were assembled together and juxtaposed to the more rigid upper plate as a result of buoyancy-driven exhumation (Fig. 9c). The older blueschists may have been incorporated into the metasediments of the middle unit during this partial exhumation. The final exhumation stage was governed by a switch from continental subduction to collision resulting in large-scale folding of the high-pressure nappe stack (Fig. 9d; Jeřábek *et al.* 2016). This stage was associated with the greenschist facies overprint of the complex at conditions of <480°C and <8.5 kbar (Žáčková *et al.* 2010), which is in our interpretation also reflected in the *c.* 334 Ma age peak in the spectrum of existing Ar–Ar data (see Fig. 13 in Žáčková *et al.* 2010). The last stage of deformation was associated with a major reorientation of the stress field that caused refolding of the exhumed and folded nappe stack by N–S oriented shortening (Jeřábek *et al.* 2016) recorded also in the southern part of the Saxothuringian Domain (Konopásek *et al.* 2001). This event took place shortly before the intrusion of the Krkonoše-Jizera pluton (Žák *et al.* 2013) and is apparently dated by the youngest *c.* 322 Ma peak in the spectrum of Ar–Ar ages (Fig. 13 in Žáčková *et al.* 2010).

Implications for existing models of the tectonic evolution of the Bohemian Massif

Current models of the Devonian–Carboniferous (Variscan) tectonic evolution in the northern (Chopin *et al.* 2012) and in the southern (Schulmann *et al.* 2014) parts of the Bohemian Massif emphasize the role of crustal relamination (Hacker *et al.* 2011; Maierová *et al.* 2018) in the evolution of the orogen. In these models, the process of subduction of the Saxothuringian oceanic crust ended before *c.* 375–370 Ma and since that time up to *c.* mid-Carboniferous, the whole Bohemian Massif evolved as a collisional orogen. The onset of continental collision was accompanied by underplating of large portions of the Saxothuringian continental crust to the bottom of the overriding Teplá-Barrandian Domain (s.l.). The main argument supporting this interpretation is the mid – late Devonian deformation, metamorphism and exhumation of the continental crust of the Teplá-Barrandian Domain (s.l.). Such early Variscan tectonic processes are documented through structural studies and extensive dating of metamorphism and cooling along the western edge of the Teplá-Barrandian Domain (s.s.) by Bowes & Aftalion (1991), Beard *et al.* (1995), Dallmeyer & Urban (1998), Bowes *et al.* (2002), Timmermann *et al.* (2004; 2006), Peřestý *et al.* (2017) and Collett *et al.* (2018). Similarly, an important Devonian (*c.* 400–370 Ma; van Breemen *et al.* 1988; O'Brien *et al.* 1997; Bröcker *et al.* 1998; Marheine *et al.* 2002; Kryza & Fanning 2007) tectonometamorphic history is recorded in the Góry Sowie unit in the northern Bohemian Massif (Fig. 1), which was interpreted as a part of the Teplá-Barrandian Domain (s.l.) by Mazur & Aleksandrowski (2001).

However, the metamorphic ages presented in this work, as well as ages for high-pressure metamorphism in the Erzgebirge in the southern Saxothuringian Domain suggest that subduction continued after the mid–late Devonian collisional event recorded in the lower–middle crust of the Teplá-Barrandian Domain (s.l.). Such a conclusion is inferred from the age of *c.* 365 Ma for the mafic blueschist of the middle unit in the Krkonoše-Jizera Complex (this work), and *c.* 340 Ma for the Erzgebirge mafic eclogites in the southern part of the Saxothuringian suture (von Quadt & Günther 1999), both regarded as metamorphosed relics of the Saxothuringian oceanic crust (Patočka & Pin 2005; Massone & Czambor 2007). The only part of the Saxothuringian suture zone without a clear

Carboniferous subduction record is its northernmost tip in the Kaczawa unit, where the age of the high-pressure metamorphism has so far not been determined.

Younger metamorphic ages related to high-pressure metamorphism of the passive margin clastic sedimentary rocks in the Krkonoše–Jizera Complex indicate that the subduction-related thermal gradient was maintained until *c.* 340 Ma, which would not be possible with the beginning of continental subduction at *c.* 375 Ma. Thus, whereas the mid–late Devonian ages of *c.* 400–370 Ma in the crustal rocks of the overriding Teplá-Barrandian Domain (s.l.) probably record a process of subduction and underplating of a small, island-like continental block, the ages of *c.* 340–337 Ma represent the youngest record of high-pressure metamorphism affecting the subducted passive margin of the Saxothuringian (s.s.) continental crust. In our view, the time interval between *c.* 370 and 340–337 Ma represents the period of the late subduction of the Saxothuringian Ocean (Fig. 9) with its final stage marking the beginning of the early Carboniferous collisional history in the Bohemian Massif.

Acknowledgement

The authors appreciate financial support by the Czech Science Foundation (GACR 17-22207S). JK thanks Martin Whitehouse and Lev Ilyinsky for their support while using the Nordsim ion probe in Stockholm (this is Nordsim publication # 578), as well as R. Škoda and R. Čopjaková from the Masaryk University in Brno for their assistance with electron microprobe analysis and imaging. The article benefited from constructive reviews by S. Mazur and José R. Martínez Catalán.

References

Aleinikoff, J.N., Schenck, W.S., Plank, M.O., Srogi, L., Fanning, C.M., Kamo, S.L. & Bosbyshell, H. 2006. Deciphering igneous and metamorphic events in high-grade rocks of the Wilmington

Complex, Delaware: Morphology, cathodoluminescence and backscattered electron zoning, and SHRIMP U–Pb geochronology of zircon and monazite. *Geological Society of America Bulletin*, **118**, 39–64.

Anczkiewicz, R., Platt, J. P., Thirlwall, M. F. & Wakabayashi, J. 2004. Franciscan subduction off to a slow start: evidence from high-precision Lu–Hf garnet ages on high grade-blocks. *Earth and Planetary Science Letters*, **225**(1-2), 147-161.

Anczkiewicz, R., Chakraborty, S., Dasgupta, S., Mukhopadhyay, D. & Koltonik, K. 2014, Timing, duration and inversion of prograde Barrovian metamorphism constrained by high resolution Lu-Hf garnet dating: A case study from the Sikkim Himalaya, NE India. *Earth and Planetary Science Letters*, **407**, 70–81.

Anczkiewicz, R., Thirlwall, M., Alard, O., Rogers, N. W. & Clark, C. 2012. Diffusional homogenization of light REE in garnet from the Day Nui Con Voi Massif in N-Vietnam: Implications for Sm-Nd geochronology and timing of metamorphism in the Red River shear zone. *Chemical Geology*, **318**, 16–30.

Beard, B.L., Medaris, L.G., Johnson, C.M., Jelínek, E., Tonika, J. & Riciputi, L.R. 1995. Geochronology and geochemistry of eclogites from the Mariánská Lázně Complex, Czech Republic: Implications for Variscan orogenesis. *Geologische Rundschau*, **84**, 552–567.

Borkowska, M., Hameurt, J. & Vidal, O. 1980. Origin and age of Izera gneisses and Rumburk granites in the West Sudetes. *Acta Geologica Polonica*, **30**, 121–145.

Bowes, D.R. & Aftalion, M. 1991. U–Pb zircon isotopic evidence for early Ordovician and late Proterozoic units in the Mariánské Lázně Complex, Central-European Hercynides. *Neues Jahrbuch für Mineralogie – Monatshefte*, **7**, 315–326.

Bowes, D.R., van Breemen, O., Hopgood, A.M. & Jelínek, E. 2002. $^{40}Ar/^{39}Ar$ isotopic evidence for mid-Devonian post-metamorphic pegmatite emplacement in the Mariánské Lázně Complex, Bohemian Massif, Central European Hercynides. *Neues Jahrbuch für Mineralogie – Monatshefte*, **10**, 445–457.

van Breemen O., Bowes D.R., Aftalion M. & Żelaźniewicz A. 1988. Devonian tectonothermal activity in the Góry Sowie gneissic block, Sudetes, southwestern Poland: evidence from Rb-Sr and U-Pb isotopic studies. *Annales Societatis Geologorum Poloniae*, **58**, 3–19.

Bröcker M., Żelaźniewicz A. & Enders M. 1998. Rb–Sr and U–Pb geochronology of migmatitic gneisses from the Góry Sowie (West Sudetes, Poland): the importance of Mid-Late Devonian metamorphism. *Journal of the Geological Society London*, **155**, 1025–1036.

Cháb, J. & Vrána, S. 1979. Crossite-actinolite amphiboles of the Krkonoše-Jizera crystalline complex and their geological significance. *Věstník Ústředního ústavu geologického*, **54**, 143–150.

Chaloupský, J. 1989. Geology of the Krkonoše and Jizerské Hory Mountains. Ústřední ústav geologický, Praha (in Czech with English summary).

Chlupáč, I. 1993. Stratigraphic evaluation of some metamorphic units in the N part of the Bohemian Massif. *Neues Jahrbuch für Geologie und Paläontologie – Abhandlungen*, **188**, 363–388.

Chopin, F., Schulmann, K., Skrzypek, E., Lehmann, J., Dujardin, J.R., Martelat, J.E., Lexa, O., Corsini, M., Edel, J.B., Štípská, P. & Pitra, P. 2012. Crustal influx, indentation, ductile thinning and gravity redistribution in a continental wedge: building a Moldanubian mantled gneiss dome with underthrust Saxothuringian material (European Variscan belt). *Tectonics*, **31**, 1–27.

Collett, S., Štípská, P., Kusbach, V., Schulmann, K. & Marciniak, G. 2017. Dynamics of Saxothuringian subduction channel/wedge constrained by phase-equilibria modelling and micro-fabric analysis. *Journal of Metamorphic Geology*, **35**, 253–280.

Collett, S., Štípská, P., Schulmann, K., Peřestý, V., Soldner, J., Anczkiewicz, R., Lexa, O. & Kylander-Clark, A. 2018. Combined Lu–Hf and Sm–Nd geochronology of the Mariánské Lázně Complex:

New constraints on the timing of eclogite- and granulite-facies metamorphism. Lithos, **304–307**, 74–94.

Corfu F. 2004. U–Pb age, setting, and tectonic significance of the anorthosite-mangerite-charnockite-granite-suite, Lofoten-Vesterålen, Norway. *Journal of Petrology*, **45**, 1799–1819.

Dallmeyer, R.D. & Urban, M. 1998. Variscan vs. Cadomian tectonothermal activity in northwestern sectors of the Teplá-Barrandian zone, Czech Republic: constraints from $^{40}Ar/^{39}Ar$ ages. *Geologische Rundschau*, **87**, 94–106.

Dostál, J., Patočka, F. & Pin, C. 2001. Middle ⁄ Late Cambrian intracontinental rifting in the central West Sudetes, NE Bohemian Massif (Czech Republic): geochemistry and petrogenesis of the bimodal metavolcanic rocks. *Geological Journal*, **36**, 1–17.

Faryad, S.W. & Kachlík V., 2013. New evidence of blueschist facies rocks and their geotectonic implication for Variscan suture(s) in the Bohemian Massif. *Journal of Metamorphic Geology*, **31**, 63–82.

Franke, W. 2000. The mid-European segment of the Variscides: tectonostratigraphic units, terrane boundaries and plate tectonic evolution. *In*: Franke, W., Haak, V., Oncken, O. & Tanner, D. (eds) *Orogenic Processes: Quantification and Modelling in the Variscan Belt*. Geological Society London Special Publication, **179**, 35–56.

Franke, W. & Żelaźniewicz, A. 2000. The eastern termination of the Variscides: terrane correlation and kinematic evolution. *In*: Franke, W., Haak, V., Oncken, O. & Tanner, D. (eds) *Orogenic Processes: Quantification and Modelling in the Variscan Belt*. Geological Society London Special Publication, **179**, 63–86.

Franke, W., Żelaźniewicz, A., Porębski & S.J., Wajsprych, B. 1993. Saxothuringian zone in Germany and in Poland: differences and common features. *Geologisch Rundschau*, **82**, 583–599.

Guiraud, M. & Burg, J. P. 1984. Mineralogical and petrological study of a blueschist metatuff from the Zelezny Brod Crystalline Complex, Czechoslovakia. *Neues Jahrbuch für Mineralogie – Abhandlungen*, **149**, 1–12.

Hacker, B.R., Kelemen, P.B. & Behn, M.D. 2011. Differentiation of the continental crust by relamination. *Earth and Planetary Science Letters*, **307**, 501e516.

Jeřábek, P., Konopásek, J. & Žáčková, E. 2016. Two-stage exhumation of subducted Saxothuringian continental crust records underplating in the subduction channel and collisional forced folding (Krkonoše-Jizera Mts., Bohemian Massif). *Journal of Structural Geology*, **89**, 214–229.

Jochum, K. P., Stoll, B., Herwig, K., Willbold, M., Hofmann, A. W., Amini, M., Aarburg, S., Abouchami, W., Hellebrand, E., Mocek, B., Raczek, I., Stracke, A., Alard, O., Bouman, C., Becker, S., Dücking, M., Brätz, H., Klemd, R., de Bruin, D., Canil, D., Cornell, D., de Hoog, C.-J., Dalpé, C., Danyushevsky, L., Eisenhauer, A., Gao, Y., Snow, J. E., Groschopf, N., Günther, D., Latkoczy, C., Guillong, M., Hauri, E. H., Höfer, H. E., Lahaye, Y., Horz, K., Jacob, D. E., Kasemann, S. A., Kent, A. J. R., Ludwig, T., Zack, T., Mason, P. R. D., Meixner, A., Rosner, M., Misawa, K., Nash, B. P., Pfänder, J., Premo, W. R., Sun, W. D., Tiepolo, M., Vannucci, R., Vennemann, T., Wayne, D. & Woodhead, J. D. 2006. MPI-DING reference glasses for in situ microanalysis: New reference values for element concentrations and isotope ratios. Geochemistry Geophysics Geosystems, 7(2).

Jochum, K. P., Weis, U., Stoll, B., Kuzmin, D., Yang, Q., Raczek, I., Jacob, D. E., Stracke, A., Birbaum, K., Frick, D. A., Günther, D. & Enzweiler, J. 2011. Determination of Reference Values for NIST SRM 610-617 Glasses Following ISO Guidelines. Geostandards and Geoanalytical Research, 35(4), 397-429.

Kachlík, V. & Kozdrój, W. 2001. Ještěd Range Unit. *In*: Kozdrój, W., Krentz, O. & Opletal, M. (eds) *Comments on the Geological map Lauzitz - Jizera - Karkonozse (without Cenozoic sediments)*. Sächsisches Landesamt für Umwelt und Geologie/Bereich Boden und Geologie, Freiberg, Panstwowy Institut Geologiczny, Warzsawa. Český geolologický ústav Praha, Warzsawa, pp. 27–31.

Kachlík, V. & Patočka, F. 1998. Cambrian ⁄ Ordovician intracontinental rifting and Devonian closure of the rifting generated basins in the Bohemian Massif realms. *Acta Universitatis Carolinae Geologica*, **42**, 433–441.

Kirkland, C.L., Whitehouse, M.J. & Slagstad, T. 2009. Fluid-assisted zircon and monazite growth within a shear zone: a case study from Finnmark, Arctic Norway. *Contributions to Mineralogy and Petrology*, **158**, 637–657.

Klápová, H., Konopásek, J. & Schulmann, K. 1998. Eclogites from the Czech part of the Erzgebirge: multi-stage metamorphic and structural evolution. Journal of the Geological Society London, **155**, 567–583.

Konopásek, J., Pilátová, E., Košler, J. & Sláma, J. 2014. Zircon (re)crystallization during short-lived, high-P granulite facies metamorphism (Eger Complex, NW Bohemian Massif). *Journal of Metamorphic Geology*, **32**, 885–902.

Konopásek, J. & Schulmann, K. 2005. Contrasting Early Carboniferous field geotherms: evidence for accretion of a thickened orogenic root and subducted Saxothuringian crust (Central European Variscides). *Journal of the Geological Society London*, **162**, 463–470.

Konopásek, J., Schulmann, K. & Lexa, O. 2001. Structural evolution of the central part of the Krušné hory (Erzgebirge) Mountains in the Czech Republic e evidence for changing stress regime during Variscan compression. *Journal of Structural Geology*, **23**, 1373–1392.

Korytowski, A., Dörr, W. & Żelaźniewicz, A. 1993. U–Pb dating of (meta)granitoids in the NW Sudetes (Poland) and their bearing on tectonostratigraphic correlation. *Terra Nova*, **5**, 331–332.

Kotková, J., Kröner, A., Todt, W. & Fiala, J. 1996. Zircon dating of North Bohemian granulites, Czech Republic: further evidence for the Lower Carboniferous high-pressure event in the Bohemian Massif. *Geologische Rundschau*, **85**, 154–161.

Kotková, J., O'Brian, P.J. & Ziemann, M.A. 2011. Diamond and coesite discovered in Saxony-type granulite: Solution to the Variscan garnet peridotite enigma. *Geology*, **39**, 667–670.

Kotková, J., Whitehouse, M., Schaltegger, U. & D'Abzac, F.X. 2016. The fate of zircon during UHT-UHP metamorphism: isotopic (U/Pb, O-18, Hf) and trace element constraints. *Journal of Metamorphic Geology*, **34**, 719–739.

Kröner, A., Hegner, E., Hammer, J., Haase, G., Bielicki, K.H., Krauss, M. & Eidam, J. 1994. Geochronology and Nd-Sr systematics of Lusatian granitoids: significance for the evolution of the Variscan orogen in east-central Europe. *Geologische Rundschau*, **83**, 357–376.

Kröner, A., Jaeckel, P., Hegner, E. & Opletal, M. 2001. Single zircon ages and wholerock Nd isotopic systematics of early Palaeozoic granitoid gneisses from the Czech and Polish Sudetes (Jizerské hory, Krkonoše and Orlice-Sněžník Complex). *International Journal of Earth Sciences*, **90**, 304–324.

Kröner, A. & Willner, A.P. 1998. Time of formation and peak of Variscan HP-HT metamorphism of quartz-feldspar rocks in the central Erzgebirge, Saxony, Germany. *Contributions to Mineralogy and Petrology*, **132**, 1–20.

Kryza, R. & Fanning, C.M. 2007. Devonian deep-crustal metamorphism and exhumation in the Variscan Orogen: evidence from SHRIMP zircon ages from the HT-HP granulites and migmatites of the Góry Sowie (Polish Sudetes). *Geodinamica Acta*, **20**, 159–175.

Kryza, R. & Mazur, S. 1995. Contrasting metamorphic paths in the SE part of the Karkonosze-Izera block (Western Sudetes, SW Poland). *Neues Jahrbuch für Mineralogie – Abhandlungen*, **169**, 157–192.

Kryza, R., Mazur, S. & Pin, C. 1995. Leszczyniec meta-igneous complex in the eastern part of the Karkonosze–Izera Block, Western Sudetes: trace element and Nd isotope study. *Neues Jahrbuch für Mineralogie – Abhandlungen*, **170**, 59–74.

Kryza, R., Muszynski, A. & Vielzeuf, D. 1990. Glaucophane-bearing assemblage overprinted by greenschist-facies metamorphism in the Variscan Kaczawa complex, Sudetes, Poland. *Journal of Metamorphic Geology*, **8**, 344–355.

Kryza, R., Schaltegger, U., Oberc-Dziedzic, T., Pin, C. & Ovtcharova, M. 2014. Geochronology of a composite granitoid pluton: a high-precision ID-TIMS U-Pb zircon study of the Variscan Karkonosze Granite (SW Poland). *International Journal of Earth Sciences*, **103**, 683–696.

Kryza, R., Zalasiewicz, J., Mazur, S., Aleksandrowski, P., Sergeev, S. & Larionov, A. 2007. Precambrian crustal contribution to the Variscan accretionary prism of the Kaczawa Mountains (Sudetes, SW Poland): evidence from SHRIMP dating of detrital zircons. *International Journal of Earth Sciences*, **96**, 1153–1162.

Lapen, T.J., Johnson, C.M., Baumgartner, L.P., Mahlen, N.J., Beard, B.L. & Amato, J.M. 2003. Burial rates during prograde metamorphism of an ultra-high-pressure terrane: an example from Lago di Cignana, western Alps, Italy. *Earth and Planetary Science Letters*, **215**, 57–72.

Ludwig, K.R. 2008. Isoplot. A Geochronological Toolkit for Microsoft Excel. Berkley Geochronology Center Special Publication No. 4.

Machowiak, K., Armstrong, R. 2007. SHRIMP U–Pb zircon age from the Karkonosze granite. Mineralogia Polonica Special Papers, **31**, 193–196.

Maierová, P., Schulmann, K., & Gerya, T. 2018. Relamination styles in collisional orogens. *Tectonics*, **37**, 224–250.

Majka, J., Mazur, S., Kosminska, K., Dudek, K. & Klonowska, I. 2016. Pressure-temperature estimates of the blueschists from the Kopina Mt., northern Bohemian Massif, Poland - constraints on subduction of the Saxothuringian continental margin. *European Journal of Mineralogy*, **28**, 1047–1057.

Maluski, H. & Patočka, F. 1997. Geochemistry and ^{40}Ar–^{39}Ar geochronology of the mafic metavolcanic rocks from the Rychory Mountains complex (west Sudetes, Bohemian Massif): palaeotectonic significance. *Geological Magazine*, **134**, 703–716.

Marheine, D., Kachlík, V., Maluski, H., Patočka, F. & Żelaźniewicz, A. 2002. The $^{40}Ar/^{39}Ar$ ages from theWest Sudetes (NE Bohemian Massif): constraints on the Variscan polyphase tectonothemal development. *In*: Winchester, J., Pharaoh, T. & Verniers, J. (eds) *Palaeozoic Amalgamation of Central Europe*, Geological Society London Special Publication, **201**, 133–155.

Massonne, H.-J. & Czambor, A. 2007. Geochemical signatures of Variscan eclogites from the Saxonian Erzgebirge, central Europe. Chemie der Erde – Geochemistry, **67**, 69–83.

Matte, P., Maluski, H., Rajlich, P. & Franke, W. 1990. Terrane boundaries in the Bohemian Massif: results of large-scale Variscan shearing. *Tectonophysics*, **177**, 151–170.

Mazur, S. & Aleksandrowski, P. 2001. The Teplá(?)/Saxothuringian suture in the Karkonosze-Izera massif, Western Sudetes, Central European Variscides. *International Journal of Earth Sciences*, 90, 341–360.

Mazur, S., Aleksandrowski, P., Kryza, R. & Oberc-Dziedzic, T. 2006. The Variscan Orogen in Poland. *Geological Quarterly*, **50**, 89–118.

Mlčoch, B., & Konopásek, J. 2010. Pre-Late Carboniferous geology along the contact of the Saxothuringian and Teplá–Barrandian zones in the area covered by younger sediments and volcanics (western Bohemian Massif, Czech Republic). *Journal of Geosciences*, **55**, 137–150.

Narębski, W. 1994. Lower to Upper Paleozoic tectonomagmatic evolution of NE part of the Bohemian Massif. *Zentralblatt für Geologie und Paläontologie*, **I**, 961–972.

Nasdala, L. & Massonne, H.J. 2000. Microdiamonds from the Saxonian Erzgebirge, Germany: in situ micro-Raman characterisation. *European Journal of Mineralogy*, **12**, 495–498.

O'Brien P.J., Kröner A., Jaeckel P., Hegner E., Żelaźniewicz A.& Kryza R. 1997. Petrological and isotopic studies on high-pressure granulites, Góry Sowie Mts., Polish Sudetes. *Journal of Petrology*, **38**, 433–456.

Oliver, G.J.H., Corfu, F. & Krogh, T.E. 1993. U–Pb ages from SW Poland: evidence for a Caledonian suture zone between Baltica and Gondwana. *Journal of the Geoleological Society London*, **150**, 355–369.

Patočka, F., Fajst, M. & Kachlík, V. 2000. Mafic-felsic to mafic–ultramafic Early Palaeozoic magmatism of the West Sudetes (NE Bohemian Massif); the South Krkonoše Complex. *Zeitschrift für Geologische Wissenschaften*, **28**, 177–210.

Patočka, F. & Pin, C. 2005. Sm–Nd isotope and trace element evidence for heterogeneous igneous protoliths of variscan mafic blueschists in the east Krkonose complex (West Sudetes, NE Bohemian Massif, Czech Republic). *Geodinamica Acta*, **18**, 363–374.

Patočka, F., Pivec, E. & Oliveriová, D. 1996. Mineralogy and petrology of mafic blueschists from the Rýchory Mts. crystalline complex (Western Sudetes, Bohemian Massif). *Neues Jahrbuch für Mineralogie – Abhandlungen*, **170**, 313–330.

Paton, C., Hellstrom, J., Paul, B., Woodhead, J., & Hergt, J. 2011. Iolite: Freeware for the visualisation and processing of mass spectrometric data. *Journal of Analytical Atomic Spectrometry*, **26**, 2508–2518.

Peřestý, V., Lexa, O., Holder, R., Jeřábek, P., Racek, M., Štípská, P., Schulmann, K. & Hacker, B. 2017. Metamorphic inheritance of Rheic passive margin evolution and its early-Variscan overprint in the Teplá-Barrandian Unit, Bohemian Massif. *Journal of Metamorphic Geology*, **35**, 327–355.

Platt, J. P., Anczkiewicz, R., Soto, J. I., Kelley, S. P. & Thirlwall, M. 2006. Early Miocene continental subduction and rapid exhumation in the western Mediterranean. *Geology*, **34**(11), 981-984.

von Quadt, A. & Günther, D. 1999. Evolution of Cambrian eclogitic rocks in the Erzgebirge: a conventional and LA-ICP-MS U-Pb zircon and Sm-Nd study. *Terra Nostra*, **99**, 164.

Scherer, E. E., Cameron, K. L. & Blichert-Toft, J. 2000. Lu–Hf garnet geochronology: closure temperature relative to the Sm–Nd system and the effects of trace mineral inclusions. *Geochimica et Cosmochimica Acta*, **64**(19), 3413-3432.

Scherer, E., Munker, C. & Mezger, K. 2001. Calibration of the lutetium–hafnium clock (vol 293, pg 683, 2001). *Science*, **293**, 1766.

Schmädicke, E., Okrusch, M. & Schmidt, W. 1992. Eclogite-facies rocks in the Saxonian Erzgebirge, Germany: high pressure metamorphism under contrasting P-T conditions. *Contributions to Mineralogy and Petrology*, **110**, 226–241.

Schulmann, K., Konopásek, J., Janoušek, V., Lexa, O., Lardeaux, J.M., Edel, J.B., Štípská, P. & Ulrich, S. 2009. An Andean type Palaeozoic convergence in the Bohemian Massif. *Comptes Rendus Geoscience*, **341**, 266–286.

Schulmann, K., Lexa, O., Janoušek, V., Lardeaux, J.M. & Edel, J.B. 2014. Anatomy of a diffuse cryptic suture zone: An example from the Bohemian Massif, European Variscides. *Geology*, **42**, 275–278.

Smulikowski, W. 1995. Evidence of glaucophane-schist facies metamorphism in the East Karkonosze complex, West Sudetes, Poland. *Geologische Rundschau*, **84**, 720–737.

Stacey, J.S. & Kramers, J.D. 1975. Approximation of terrestrial lead isotope evolution by a 2-stage model. *Earth and Planetary Science Letters*, **26**, 207–221.

Steiger, R.H. & Jager, E. 1977. Subcommission on geochronology: Convention on the use of decay constants in geo- and cosmochronology. *Earth and Planetary Science Letters*, **36**, 359–362.

Stosch, H. & Lugmair, G. 1990. Geochemistry and evolution of MORB-type eclogites from the Münchberg Massif, southern Germany. *Earth and Planetary Science Letters*, **99**, 230–249.

Sun, S.-S. & McDonough, W. 1989. Chemical and isotopic systematics of oceanic basalts: implications for mantle composition and processes. *Geological Society, London, Special Publications*, **42**(1), 313-345.

Tichomirowa, M., Berger, H.-J., Koch, E. A., Belyatski, B. V., Gotze, J., Kempe, U., Nasdala, L. & Schaltegger, U. 2001. Zircon ages of high-grade gneisses in the Eastern Erzgebirge (Central European Variscides) – constraints on origin of the rocks and Precambrian to Ordovician magmatic events in the Variscan foldbelt. *Lithos*, **56**, 303–32.

Timmermann, H., Dörr, W., Krenn, E., Finger, F. & Zulauf, G. 2006. Conventional and in situ geochronology of the Teplá Crystalline unit, Bohemian Massif: implications for the processes involving monazite formation. *International Journal of Earth Sciences*, **95**, 629–647.

Timmermann, H., Štědrá, V., Gerdes. A., Noble, S.R., Parrish, R.R. & Dörr, W. 2004. The problem of dating high-pressure metamorphism: a U-Pb isotope and geochemical study on eclogites and related rocks of the Mariánské Lázně Complex, Czech Republic. *Journal of Petrology*, **45**, 1311–1338.

Van Achterbergh, E., Ryan, C.G., Jackson, S.E. & Griffin, W.L. 2001. Data reduction software for LA-ICP-MS: appendix. *In:* Sylvester, P.J. (ed) *Laser Ablation-ICP-Mass Spectrometry in the Earth Sciences: Principles and Applications* Mineralogical Association of Canada (MAC) Short Course Series, Ottawa, Ontario, Canada, **29**, 239 – 243.

Werner, O. & Lippolt, H.J. 2000. White mica $^{40}Ar/^{39}Ar$ ages of Erzgebirge metamorphic rocks: simulating the chronological results by a model of Variscan crustal imbrication. *In*: Franke, W., Haak, V., Oncken, O. & Tanner, D. (eds) *Orogenic Processes: Quantification and Modelling in the Variscan Belt*. Geological Society London Special Publication, **179**, 323–336.

Whitehouse, M.J. & Kamber, B. 2005. Assigning dates to thin gneissic veins in high-grade metamorphic terranes: a cautionary tale from Akilia, southwest Greenland. *Journal of Petrology*, **46**, 291–318.

Winchester, J.A., Floyd, P.A., Chocyk, M., Horbowy, K. & Kozdrój, W. 1995. Geochemistry and tectonic environment of Ordovician meta-igneous rocks in the Rudawy Janowickie Complex, SW Poland. *Journal of the Geological Society London*, **152**, 105–115.

Winchester, J.A., Patočka, F., Kachlík, V., Melzer, M., Nawakowski, C., Crowley, Q.G. & Floyd, P.A. 2003. Geochemical discrimination of metasedimentary sequences in the Krkonose–Jizera Terrane (West Sudetes, Bohemian Massif): Paleotectonic and stratigraphic constraints. *Geologica Carpathica*, **54**, 267–280.

Woodhead, J. D., Hellstrom, J., Hergt, J. M., Greig, A. & Maas, R. 2007. Isotopic and Elemental Imaging of Geological Materials by Laser Ablation Inductively Coupled Plasma-Mass Spectrometry. *Geostandards and Geoanalytical Research*, **31**, 331–343.

Zulauf, G., Dörr, W., Fiala, J., Kotková, J., Maluski, H. & Valverde-Vaquero, P. 2002. Evidence for high-temperature diffusional creep preserved by rapid cooling of lower crust (North Bohemian shear zone, Czech Republic). *Terra Nova*, **14**, 343–354.

Žáčková, E., Konopásek, J., Jeřábek, P., Finger, F. & Košler, J. 2010. Early Carboniferous blueschist-facies metamorphism in metapelites of the West Sudetes (Northern Saxothuringian Domain, Bohemian Massif). *Journal of Metamorphic Geology*, **28**, 361–379.

Žáčková, E., Konopásek, J., Košler, J. & Jeřábek, P. & 2012. Detrital zircon populations in quartzites of the Krkonoše-Jizera Massif: implications for pre-collisional history of the Saxothuringian Domain in the Bohemian Massif. *Geological Magazine*, **149**, 443–458.

Žák, J., Verner, K., Sláma, J., Kachlík, V. & Chlupáčová, M. 2013. Multistage magma emplacement and progressive strain accumulation in the shallow-level Krkonoše-Jizera plutonic complex, Bohemian Massif. *Tectonics*, **32**, 1493–1512.

Appendix – analytical methods

SIMS monazite U–Pb dating

Prior to the SIMS analysis, the samples were mounted in epoxy, coated with c. 30 nm of gold and analysed for isotopes of U, Pb and interfering molecules on a Cameca IMS 1280 ion probe at the Swedish Museum of Natural History in Stockholm (Nordsim facility). The instrument parameters, analytical method, calibration and correction procedures were similar to those described by Whitehouse & Kamber (2005) and Kirkland *et al.* (2009). The instrument was operated in automated mode with *c.* 18 μm ion beam diameter. The measured Pb/U ratios were calibrated against the reference monazite from a metapelite of the Wilmington Complex, Delaware, which has a TIMS age of 424.9 ± 0.4 Ma (sample 44069; Aleinikoff *et al.* 2006). Common lead corrections assuming a modern-day average terrestrial common Pb composition (Stacey & Kramers 1975) were made only when ^{204}Pb counts statistically exceeded average background.

ID-TIMS monazite U–Pb dating

The monazite grains selected for analysis were cleaned in hot HNO_3 and rinsed in H_2O and acetone, combined with an ultrasonic treatment. They were dissolved in 6N HCl on a hot-plate, after adding a mixed ^{202}Pb-^{205}Pb-^{235}U spike, and processed in ion-exchange resin to purify Pb and U. The isotopic ratios were obtained with a MAT262 mass spectrometer using both static Faraday and dynamic secondary electron multiplier measurements. The data are corrected for blanks of 2 pg Pb and 0.1 pg U and using a composition calculated with the model of Stacey & Kramers (1975) for the remaining initial Pb (highest in the discordant point at 9.1 pg). The spike is calibrated against the ET100 solution, decay constants and U composition are those recommended by Steiger & Jäger (1977). Other details of the dating method are summarized in Corfu (2004).

Lu–Hf garnet dating

Lu–Hf garnet geochronology and trace element measurements were carried out at the Institute of Geological Sciences, Polish Academy of Sciences, Krakow Research Centre. Details of isotope dilution Lu–Hf analyses are described in Anczkiewicz *et al.* (2014) and references therein. Normalizing values, standard reproducibility and constants used for calculations are given in the footnote to Tab. 3. Isochron age calculations were conducted using Isoplot 4 (Ludwig 2008). Ages are given with 2σ uncertainties. Description of the apparatus and methodological details of laser ablation ICP-MS trace element measurements are provided in Anczkiewicz *et al.* (2012). NIST 612 was used as a primary standard and MPI DING glasses were measured for quality control. Reference values for the standard materials were adopted from Jochum *et al.* (2006) and Jochum *et al.* (2011). Trace element measurements in garnet were conducted in raster mode, while monazite was analysed in stationary mode with a spot size of 20 µm. Silica content was used as an internal standard for garnet and Ce content obtained by microprobe analyses was used as an internal standard for monazite. Abundance of trace elements was calculated using Iolite 3 (Paton *et al.* 2011; Woodhead *et al.* 2007) and Glitter (Van Achterbergh *et al.* 2001) software.

Figure and table captions:

Fig. 1 – Simplified geological map of the Bohemian Massif (modified after Franke 2000). The position of the study area is shown as a black rectangle in the northern part of the map. Abbreviations: GS - Góry Sowie unit, LC – Leszczyniec Complex.

Fig. 2 – Simplified geological map of the southern Krkonoše-Jizera Massif (modified after Chaloupský, 1989) showing the location of the samples dated in this study (black squares) and of petrological samples studied by Žáčková *et al.* (2010) and Jeřábek *et al.* (2016).

Fig. 3 – Back-scattered electron images of the dated samples VU 602, EL 9/2 and VU 601 showing their mineral assemblages. Abbreviations: Ms – pottasic white mica, Grt – garnet, Bt – biotite, Ilm – ilmenite, Qtz – quartz, Mnz – monazite, Cld – chloritoid, Chl – chlorite, Ca-Amp – calcic clinoamphibole, Gla – glaucophane, Ep – epidote, Ttn – titanite.

Fig. 4 – Compositional maps of monazite crystals from samples VU 602 and EL 9/2 showing chemical zonation in Th, Nd, Gd and La content.

Fig. 5 – U–Pb concordia plots for the monazite samples dated in this study. Error ellipses are plotted at 2σ level. MSWD – mean square of weighted derivatives. Grey and dashed ellipse in fig. b) represents one analysis not involved in the age calculation.

Fig. 6 – Lu–Hf isochron plots of dated samples. Symbols are larger than analytical uncertainties. $I_{176/177}$ refers to initial $^{176}Hf/^{177}Hf$ ratio.

Fig. 7 – Element zonation profiles of Lu, Hf, Y, U, Ti and P measured by LA ICP–MS across garnet crystals in samples (a–c) VU 602, (d–f) VU 600 and (g–i) VU 601E.

Fig. 8 – Chondrite normalized diagrams of the REE composition of dated monazites and garnets from sample VU 602. Normalizing values are from Sun & McDonough (1989).

Fig. 9 – Interpretative succession of events in the Saxothuringian subduction channel. (a) Dating of mafic blueschists at *c.* 365 Ma suggests re-establishment of oceanic subduction after relamination of continental crust at *c.* 380–370 Ma, as inferred by Chopin *et al.* (2012). (b) Subduction of thinned Saxothuringian continental margin at *c.* 345–337 Ma, which is suggested by the age of high-pressure metamorphism in the metasedimentary rocks of the lower and middle units. (c) Onset of the continental collision stage at *c.* 337 Ma. (d) Collisional forced folding at the late stage of convergence (Jeřábek *et al.* 2016).

Tab. 1 – Representative microprobe analyses of monazites.

Tab. 2 – Analytical data for the monazite samples VU 602A and EL 9/2.

Tab. 3 – Results of Lu–Hf garnet dating.

Footnote to Tab. 3

Uncertainties on Hf isotope ratios are 2SE (standard errors) and refer to the last significant digits. $^{176}Lu/^{177}Hf$ errors are 0.5%. Reproducibility of $^{176}Hf/^{177}Hf$ for JMC475 Hf standard yielded 0.282159 ± 6 2SD (standard deviation) over the period of analyses (n=7). Mass bias correction to $^{179}Hf/^{177}Hf$=0.7325. Decay constant λ_{176Lu}=1.865× 10–11 yr^{-1} (Scherer *et al.* 2001). Age calculations conducted using Isoplot v. 4.15 (Ludwig 2008). Age uncertainties are 2σ.

Tab. 4 – Results of LA ICP-MS trace element abundance measurements in monazite and garnet from sample VU 602.

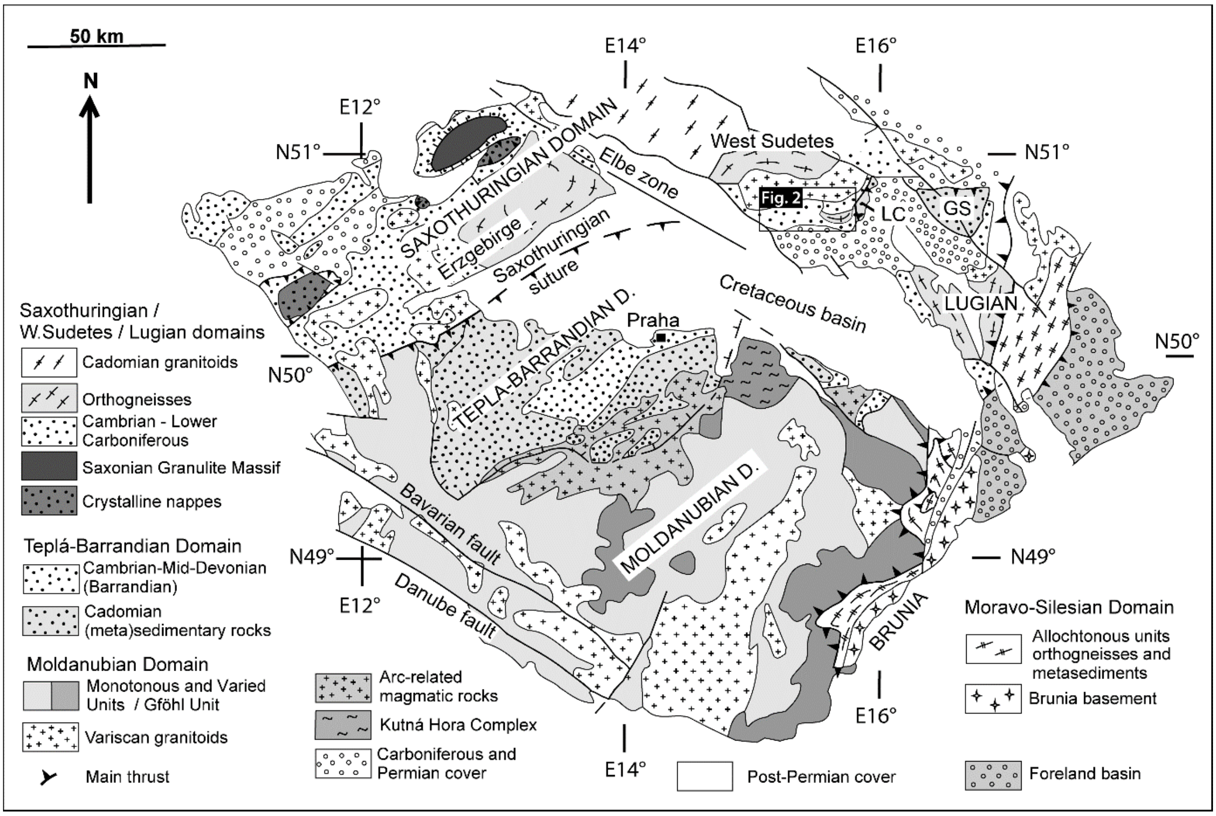
50 km
N
E14°
E16°
E12°
N51°
N51°
SAXOTHURINGIAN DOMAIN
Elbe zone
West Sudetes
Fig. 2
LC
GS
Erzgebirge
Saxothuringian suture
Cretaceous basin
LUGIAN
N50°
N50°
TEPLA-BARRANDIAN D.
Praha
MOLDANUBIAN D.
Bavarian fault
Danube fault
N49°
N49°
E12°
BRUNIA
E16°
E14°
Saxothuringian / W.Sudetes / Lugian domains
Cadomian granitoids
Orthogneisses
Cambrian - Lower Carboniferous
Saxonian Granulite Massif
Crystalline nappes
Teplá-Barrandian Domain
Cambrian-Mid-Devonian (Barrandian)
Cadomian (meta)sedimentary rocks
Moldanubian Domain
Monotonous and Varied Units / Gföhl Unit
Variscan granitoids
Main thrust
Arc-related magmatic rocks
Kutná Hora Complex
Carboniferous and Permian cover
Post-Permian cover
Moravo-Silesian Domain
Allochtonous units orthogneisses and metasediments
Brunia basement
Foreland basin

Fig.1

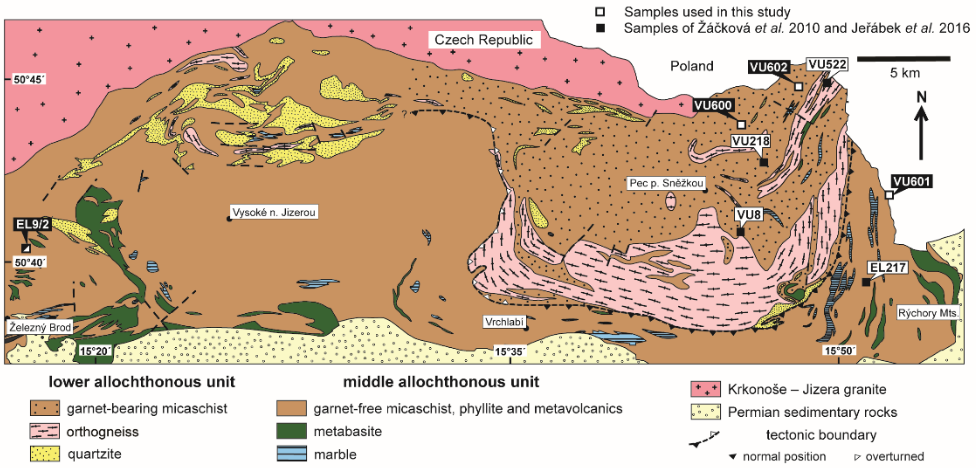
Samples used in this study
Samples of Žáčková et al. 2010 and Jeřábek et al. 2016
Czech Republic
Poland
5 km
N
50°45'
50°40'
VU602
VU522
VU600
VU218
VU601
VU8
EL217
EL9/2
Pec p. Sněžkou
Vysoké n. Jizerou
Železný Brod
Vrchlabí
Rýchory Mts.
15°20'
15°35'
15°50'
lower allochthonous unit
garnet-bearing micaschist
orthogneiss
quartzite
middle allochthonous unit
garnet-free micaschist, phyllite and metavolcanics
metabasite
marble
Krkonoše – Jizera granite
Permian sedimentary rocks
tectonic boundary
normal position
overturned

Fig.2

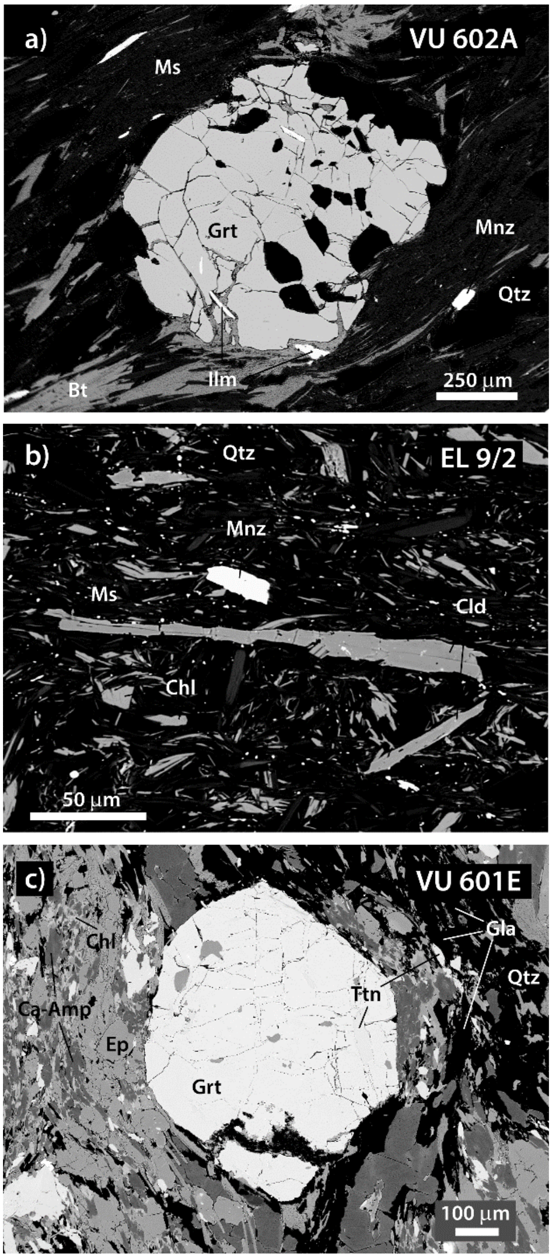
a)
VU 602A
Ms
Grt
Mnz
Qtz
Bt
Ilm
250 µm
b)
Qtz
EL 9/2
Mnz
Ms
Cld
Chl
50 µm
c)
VU 601E
Chl
Gla
Qtz
Ttn
Ca-Amp
Ep
Grt
100 µm

Fig.3

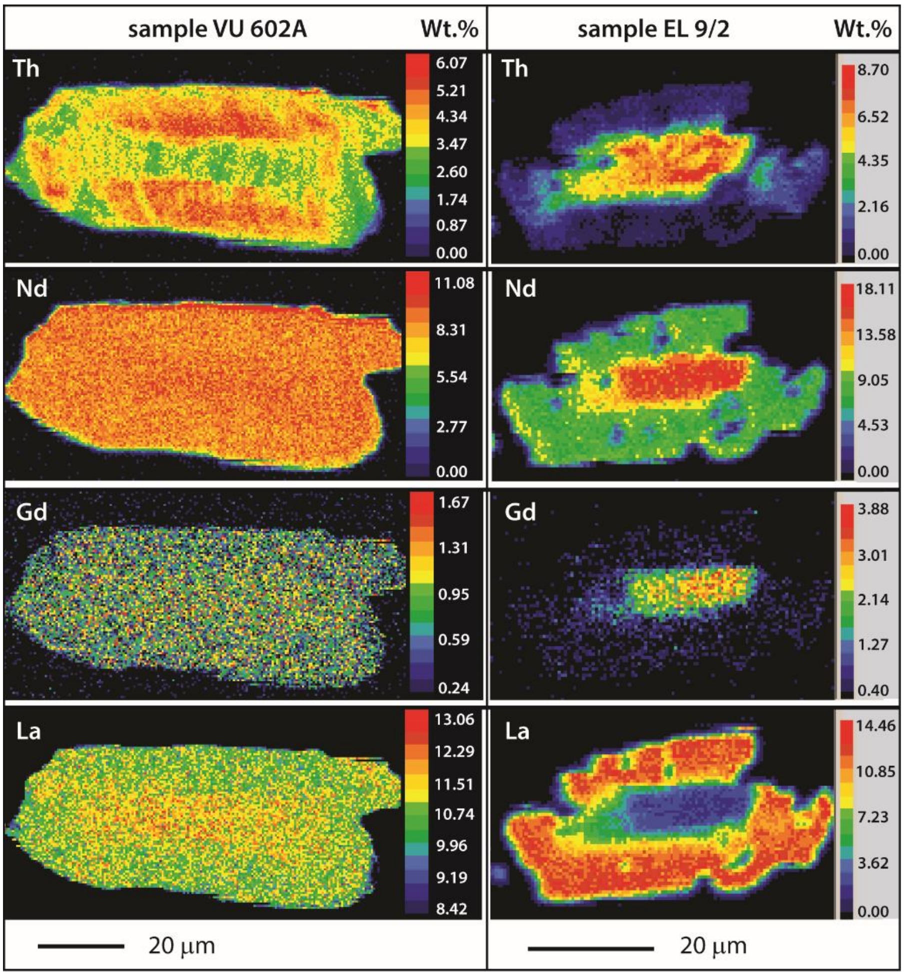
sample VU 602A
Wt.%
sample EL 9/2
Wt.%
Th
6.07
5.21
4.34
3.47
2.60
1.74
0.87
0.00
Th
8.70
6.52
4.35
2.16
0.00
Nd
11.08
8.31
5.54
2.77
0.00
Nd
18.11
13.58
9.05
4.53
0.00
Gd
1.67
1.31
0.95
0.59
0.24
Gd
3.88
3.01
2.14
1.27
0.40
La
13.06
12.29
11.51
10.74
9.96
9.19
8.42
La
14.46
10.85
7.23
3.62
0.00
20 μm
20 μm

Fig.4

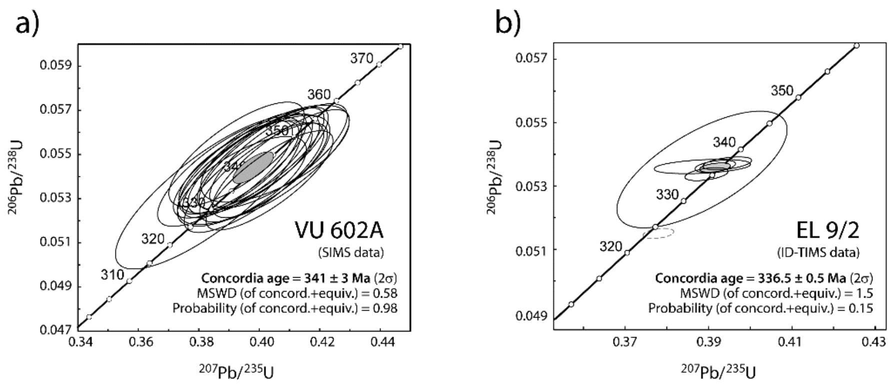
a)
b)
0.059
0.057
0.055
0.053
0.051
0.049
0.047
0.34
0.36
0.38
0.40
0.42
0.44
370
360
350
330
320
310
$^{206}Pb/^{238}U$
$^{207}Pb/^{235}U$
VU 602A
(SIMS data)
Concordia age = 341 ± 3 Ma (2σ)
MSWD (of concord.+equiv.) = 0.58
Probability (of concord.+equiv.) = 0.98
0.057
0.055
0.053
0.051
0.049
0.37
0.39
0.41
0.43
350
340
330
320
$^{206}Pb/^{238}U$
$^{207}Pb/^{235}U$
EL 9/2
(ID-TIMS data)
Concordia age = 336.5 ± 0.5 Ma (2σ)
MSWD (of concord.+equiv.) = 1.5
Probability (of concord.+equiv.) = 0.15

Fig.5

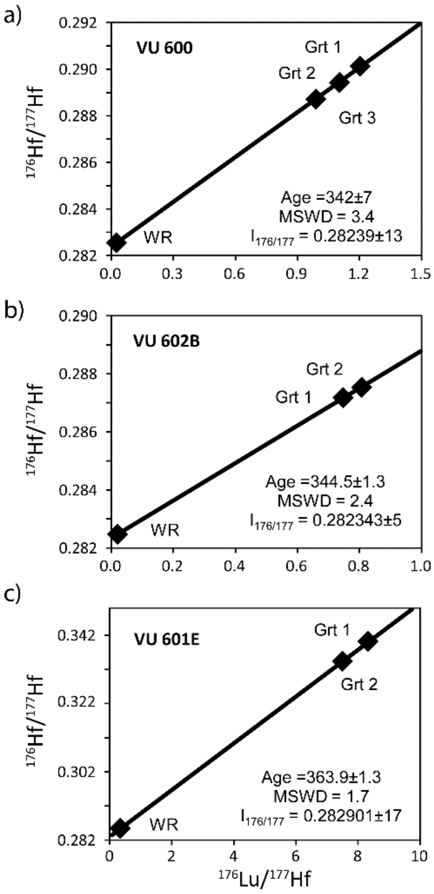
a)
VU 600
Grt 1
Grt 2
Grt 3
WR
Age =342±7
MSWD = 3.4
I176/177 = 0.28239±13
176Hf/177Hf
b)
VU 602B
Grt 2
Grt 1
WR
Age =344.5±1.3
MSWD = 2.4
I176/177 = 0.282343±5
176Hf/177Hf
c)
VU 601E
Grt 1
Grt 2
WR
Age =363.9±1.3
MSWD = 1.7
I176/177 = 0.282901±17
176Hf/177Hf
176Lu/177Hf

Fig.6

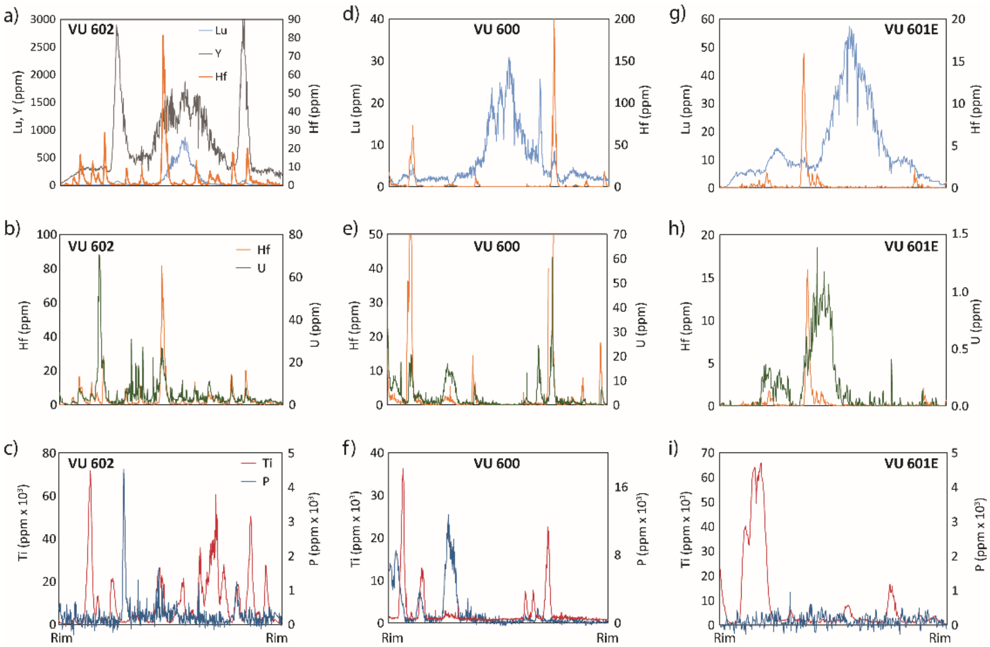
a)
VU 602
Lu
Y
Hf
Lu, Y (ppm)
Hf (ppm)
d)
VU 600
Lu (ppm)
Hf (ppm)
g)
VU 601E
Lu (ppm)
Hf (ppm)
b)
VU 602
Hf
U
Hf (ppm)
U (ppm)
e)
VU 600
Hf (ppm)
U (ppm)
h)
VU 601E
Hf (ppm)
U (ppm)
c)
VU 602
Ti
P
Ti (ppm x 10³)
P (ppm x 10³)
f)
VU 600
Ti (ppm x 10³)
P (ppm x 10³)
i)
VU 601E
Ti (ppm x 10³)
P (ppm x 10³)
Rim
Rim

Fig.7

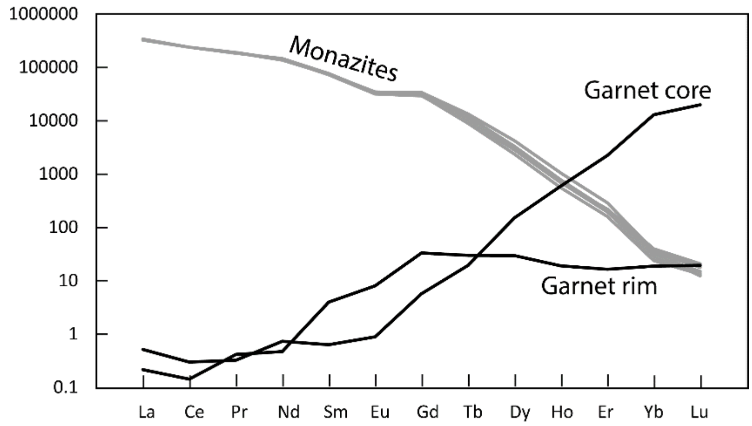
1000000
100000
10000
1000
100
10
1
0.1
Monazites
Garnet core
Garnet rim
La
Ce
Pr
Nd
Sm
Eu
Gd
Tb
Dy
Ho
Er
Yb
Lu

Fig.8

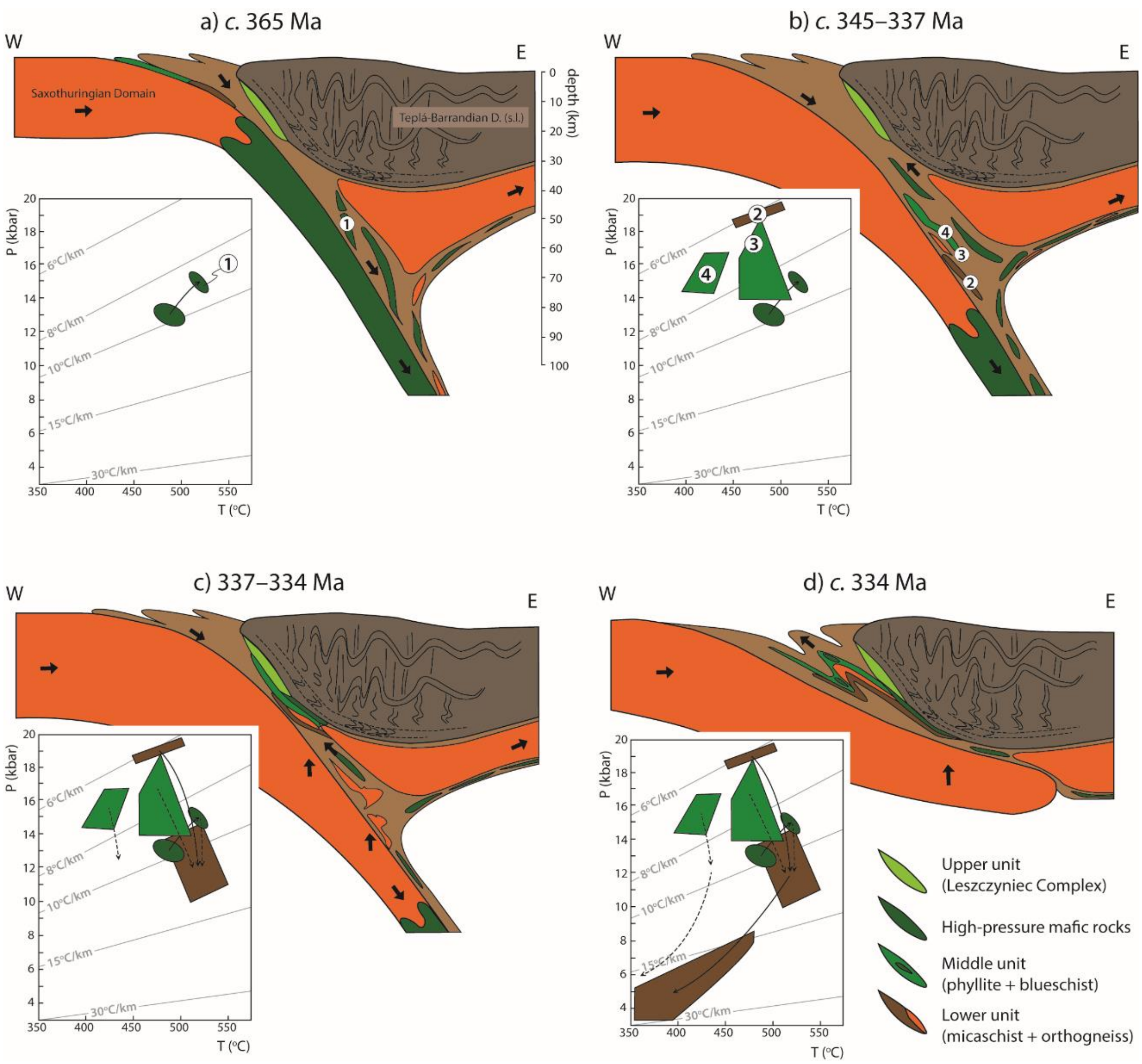
a) c. 365 Ma
b) c. 345–337 Ma
c) 337–334 Ma
d) c. 334 Ma
W
E
Saxothuringian Domain
Teplá-Barrandian D. (s.l.)
depth (km)
P (kbar)
T (°C)
6°C/km
8°C/km
10°C/km
15°C/km
30°C/km
Upper unit
(Leszczyniec Complex)
High-pressure mafic rocks
Middle unit
(phyllite + blueschist)
Lower unit
(micaschist + orthogneiss)

Fig.9

Table 1. Representative microprobe analyses of monazites

Sample	VU 602A	VU 602A	EL9/2	EL9/2
	Mnz BSE-bright	Mnz BSE-dark	Mnz core	Mnz rim
Wt%				
P_2O_5	29.83	30.20	29.58	30.49
SiO_2	0.43	0.17	0.72	0.19
UO_2	0.43	0.29	0.15	0.08
ThO_2	6.36	2.78	7.97	2.22
La_2O_3	14.92	15.58	3.43	16.92
Ce_2O_3	28.10	30.75	17.19	31.25
Pr_2O_3	3.05	3.28	3.70	3.24
Nd_2O_3	11.20	11.72	21.53	11.06
Sm_2O_3	2.02	2.00	7.56	1.66
Eu_2O_3	0.34	0.36	1.34	0.23
Gd_2O_3	1.05	1.06	3.86	0.53
Dy_2O_3	0.09	0.13	0.48	0.17
Y_2O_3	0.12	0.14	0.70	0.58
PbO	0.09	0.05	0.09	0.07
CaO	1.04	0.56	1.11	0.39
Total	99.05	99.07	99.42	99.08

Table 1

Tab. 2 - Analytical data and calculated ages for the monazite samples VU 602A and EL 9/2.

	ISOTOPIC RATIOS								ELEMENT CONCENTRATIONS			CALCULATED AGES Ma					
Analysis	$^{207}Pb/^{235}U$	± 1 sigma (%)	$^{206}Pb/^{238}U$	± 1 sigma (%)	Rho	$^{207}Pb/^{206}Pb$	± 1 sigma (%)	$^{206}Pb/^{204}Pb$	U (ppm)	Th (ppm)	Pb (ppm)	$^{207}Pb/^{235}U$	± 1 sigma	$^{206}Pb/^{238}U$	± 1 sigma	$^{207}Pb/^{206}Pb$	± 1 sigma
									Sample VU 602A – SIMS data								
# 1	0.3924	2.1632	0.0543	1.6554	0.77	0.0524	1.3925	4958	3237	40469	823	336	6	341	6	302	31
# 2	0.3945	2.1768	0.0546	1.7189	0.79	0.0524	1.3357	5203	3068	34804	725	338	6	343	6	303	30
# 3	0.3983	2.3691	0.0540	1.8839	0.80	0.0535	1.4365	3812	3881	52406	823	340	7	339	6	352	32
# 4	0.3887	2.3456	0.0541	1.8124	0.77	0.0521	1.4890	3170	2937	20809	855	333	7	340	6	288	34
# 5	0.4014	2.1524	0.0542	1.6907	0.79	0.0537	1.3320	5099	3438	52647	855	343	6	340	6	360	30
# 6	0.3962	2.2182	0.0545	1.7657	0.80	0.0527	1.3426	5149	3419	18151	800	339	6	342	6	317	30
# 7	0.3954	2.2792	0.0544	1.5744	0.69	0.0527	1.6480	4719	3613	34387	1004	338	7	342	5	315	37
# 8	0.4005	2.1438	0.0548	1.7055	0.80	0.0530	1.2989	7441	3821	53133	624	342	6	344	6	328	29
# 9	0.4064	2.2843	0.0549	1.7528	0.77	0.0536	1.4648	5690	2913	39542	841	346	7	345	6	356	33
# 10	0.4072	2.2763	0.0546	1.8318	0.80	0.0541	1.3513	8482	3738	50385	516	347	7	343	6	375	30
# 11	0.4034	2.1310	0.0538	1.7074	0.80	0.0544	1.2750	5690	3653	24469	727	344	6	338	6	386	28
# 12	0.3833	3.2848	0.0533	2.6444	0.81	0.0522	1.9486	3011	2869	34550	781	329	9	334	9	294	44
# 13	0.3943	2.2092	0.0538	1.5463	0.70	0.0532	1.5778	4792	3633	53535	1018	337	6	338	5	336	35
# 14	0.3982	2.5862	0.0543	1.8599	0.72	0.0532	1.7970	3861	3265	37504	874	340	8	341	6	337	40
# 15	0.3982	2.2341	0.0546	1.7021	0.76	0.0529	1.4470	7707	4074	479674	708	340	6	342	6	326	33
# 16	0.4052	2.4742	0.0550	1.6321	0.66	0.0534	1.8596	6459	3043	39911	754	345	7	345	5	346	42
# 17	0.4014	2.1784	0.0548	1.7361	0.80	0.0531	1.3159	4893	2983	363813	806	343	6	344	6	334	30
# 18	0.3925	2.3320	0.0550	1.7556	0.75	0.0518	1.5349	4136	3256	706976	780	336	7	345	6	275	35

	ISOTOPIC RATIOS								ELEMENT CONCENTRATIONS			CALCULATED AGES Ma					
Analysis	$^{207}Pb/^{235}U$	± 2 sigma (abs)	$^{206}Pb/^{238}U$	± 2 sigma (abs)	Rho	$^{207}Pb/^{206}Pb$	± 2 sigma (abs)	$^{206}Pb/^{204}Pb$	U (ppm)	Th (ppm)	Pb (ppm)	$^{207}Pb/^{235}U$	± 2 sigma	$^{206}Pb/^{238}U$	± 2 sigma	$^{207}Pb/^{206}Pb$	± 2 sigma
									Sample EL 9/2 – ID-TIMS data								
# 1	0.3945	0.0047	0.0537	0.0002	0.49	0.0533	0.0006	461	387	10110	171	337.6	3.4	337.3	1.0	340.0	24.3
# 2	0.3916	0.0039	0.0536	0.0001	0.46	0.0530	0.0005	383	638	37761	603	335.5	2.8	336.7	0.9	327.4	20.3
# 3	0.3885	0.0094	0.0536	0.0002	0.35	0.0526	0.0012	152	269	10521	176	333.3	6.8	336.7	1.1	309.7	51.9
# 4	0.3895	0.0042	0.0534	0.0002	0.47	0.0529	0.0005	379	499	24048	387	334.0	3.0	335.2	1.0	325.8	21.8
# 5	0.3884	0.0166	0.0535	0.0015	0.69	0.0526	0.0016	319	737	37123	600	333.2	12.1	336.1	9.1	313.1	69.4
# 6	*0.3783*	*0.0029*	*0.0515*	*0.0001*	*0.39*	*0.0533*	*0.0004*	*447*	*491*	*24582*	*365*	*325.8*	*2.2*	*323.8*	*0.7*	*340.3*	*16.2*

Data shown in *italics* were not used for the calculation of the age.

Table 2

Tab. 2 - Results of Lu-Hf garnet dating.

Sample	Fraction	Weight [mg]	Lu [ppm]	Hf [ppm]	$^{176}Lu/^{177}Hf$	$^{176}Hf/^{177}Hf$	Age [Ma]
VU 600	GRT1	73.78	15.02	1.77	1.2032	0.290134±6	**342±7**
VU 600	GRT2	79.17	14.18	1.82	1.1027	0.289424±4	
VU 600	GRT3	70.01	13.34	1.91	0.9893	0.288714±8	
VU 600	WR	99.95	0.52	2.91	0.0252	0.282550±5	
VU 601E	GRT1	74.49	6.50	0.11	8.3195	0.339753±18	**363.9±1.9**
VU 601E	GRT2	68.80	6.54	0.12	7.5003	0.333918±17	
VU 601E	WR	99.78	0.76	0.32	0.3350	0.285185±8	
VU 602	GRT1	72.09	7.03	1.33	0.7476	0.287181±6	**344.5±1.3**
VU 602	GRT2	68.14	7.63	1.34	0.8068	0.287535±5	
VU 602	WR	99.98	0.37	2.68	0.0197	0.282470±5	

Uncertainties on Hf isotope ratios are 2SE (standard errors) and refer to the last significant digits. $^{176}Lu/^{177}Hf$ errors are 0.5%. Reproducibility of $^{176}Hf/^{177}Hf$ for JMC475 Hf standard yielded 0.282159 ± 6 2SD (standard deviation) over the period of analyses (n=7). Mass bias correction to $^{179}Hf/^{177}Hf$ = 0.7325 Decay constant λ_{176Lu}=1.865× 10^{-11} yr^{-1} (Scherer *et al.* 2001). Age calculations conducted using Isoplot v. 4.15 (Ludwig 2008). Age uncertainties are 2σ.

Table 3

Table 4. Results of LA ICP-MS trace element abundance (ppm) measurements in monazite (m) and garnet (Grt) from sample VU 602.

Element	m1 core	m1 rim	m2 rim	m3 rim	m4 core	m5 core	m6 rim	m7 core	Grt core	Grt rim
^{89}Y	1388	1298	1452	1999	1281	1036	1436	1361	1508	48
^{139}La	125178	118971	119667	119943	120177	121656	121607	120352	0.19	0.08
^{140}Ce	228759	228759	228759	228759	228759	228759	228759	228759	0.28	0.14
^{141}Pr	25295	25476	25846	25956	25605	26097	25887	25787	0.04	0.06
^{146}Nd	104331	101105	101287	101113	100544	101049	99666	97614	0.52	0.33
^{147}Sm	17810	16743	17597	17428	17322	17186	17347	17102	0.15	0.92
^{153}Eu	2967	2741	2943	2956	2892	2836	3008	2905	0.08	0.70
^{157}Gd	10243	8935	10393	10429	9528	9165	10018	9826	1.74	10.19
^{159}Tb	608	581	684	779	588	518	646	633	1.13	1.72
^{163}Dy	1129	1076	1268	1608	1074	898	1173	1162	57.40	11.24
^{165}Ho	62	59	66	89	59	47	62	62	50.61	1.62
^{166}Er	51	55	53	72	48	40	50	49	556	4.08
^{172}Yb	7.5	9.8	7.6	9.1	7.7	5.9	8.0	6.9	3222	4.66
^{175}Lu	0.6	0.8	0.5	0.7	0.5	0.5	0.7	0.5	754	0.74

Table 4